Photoreceptor Cells With Profound Structural Deficits Can Support Useful Vision in Mice

Stewart Thompson,[1,2] Frederick R. Blodi,[1–3] Swan Lee,[1,2] Chris R. Welder,[1,2] Robert F. Mullins,[1,2] Budd A. Tucker,[1,2] Steven F. Stasheff,[1–3] and Edwin M. Stone[1,2,4]

[1]Department of Ophthalmology and Visual Sciences, University of Iowa, Iowa City, Iowa
[2]The Stephen A. Wynn Institute for Vision Research, University of Iowa, Iowa City, Iowa
[3]Department of Pediatrics, University of Iowa, Iowa City, Iowa
[4]Howard Hughes Medical Institute, University of Iowa, Iowa City, Iowa

Correspondence: Stewart Thompson, 4136 MERF, 375 Newton Road, Iowa City, Iowa 52242; stewart-thompson@uiowa.edu.

Submitted: November 26, 2013
Accepted: February 14, 2014

Citation: Thompson S, Blodi FR, Lee S, et al. Photoreceptor cells with profound structural deficits can support useful vision in mice. *Invest Ophthalmol Vis Sci*. 2014;55:1859–1866. DOI:10.1167/iovs.13-13661

Purpose. In animal models of degenerative photoreceptor disease, there has been some success in restoring photoreception by transplanting stem cell–derived photoreceptor cells into the subretinal space. However, only a small proportion of transplanted cells develop extended outer segments, considered critical for photoreceptor cell function. The purpose of this study was to determine whether photoreceptor cells that lack a fully formed outer segment could usefully contribute to vision.

Methods. Retinal and visual function was tested in wild-type and *Rds* mice at 90 days of age (*Rds*^{P90}). Photoreceptor cells of mice homozygous for the *Rds* mutation in peripherin 2 never develop a fully formed outer segment. The electroretinogram and multielectrode recording of retinal ganglion cells were used to test retinal responses to light. Three distinct visual behaviors were used to assess visual capabilities: the optokinetic tracking response, the discrimination-based visual water task, and a measure of the effect of vision on wheel running.

Results. *Rds*^{P90} mice had reduced but measurable electroretinogram responses to light, and exhibited light-evoked responses in multiple types of retinal ganglion cells, the output neurons of the retina. In optokinetic and discrimination-based tests, acuity was measurable but reduced, most notably when contrast was decreased. The wheel running test showed that *Rds*^{P90} mice needed 3 log units brighter luminance than wild type to support useful vision (10 cd/m^2).

Conclusions. Photoreceptors that lack fully formed outer segments can support useful vision. This challenges the idea that normal cellular structure needs to be completely reproduced for transplanted cells to contribute to useful vision.

Keywords: mouse, photoreceptor, retinal degeneration, stem cell, visual behavior

Damage to the rod and cone photoreceptor cells causes loss of vision in blinding diseases such as retinitis pigmentosa and macular degeneration.[1–3] Photoreceptor cell input to downstream neural circuits of the retina plays a key role in encoding specific features of the visual environment (movement, color, contrast, and irradiance) and the spatial relationships of visual features.[4,5] This means that the ideal solution for restoring vision in photoreceptor degenerations is to restore photoreception at the outer retina.

If significant outer retinal structure remains, stem cell–derived photoreceptor cells introduced to the subretinal space can orient appropriately, make synaptic connections, form outer segments, and respond to light.[6–13] However, in advanced photoreceptor degeneration, only a minority of transplanted cells develop a fully formed outer segment.[7,11,12,14,15] The outer segment houses the cellular machinery that initiates the response to light and is considered a critical feature of the photoreceptor cells. As stem cell–based therapies will likely be initially directed at severely degenerated retinas, it will be important to determine whether lack of a fully formed outer segment will prevent or limit a contribution to functional vision.

Mice homozygous for the *Rds* allele of peripherin 2 never develop fully formed outer segments.[16–21] Instead they have a cilia protrusion from the inner segment, with a concentration of opsin at the apical tip of the cell, but no discs or lamellae.[16,18,19,22,23] Despite the structural deficit, electrophysiological recordings suggest that *Rds* photoreceptor cells generate a response to light.[24]

The gross similarity in structural deficit of *Rds* and stem cell–derived photoreceptors presents a model to determine whether lack of a fully formed outer segment precludes a useful role in vision.[12,21] The caveats in this approach are that *Rds* photoreceptors may be more numerous and better integrated than a stem cell transplantation. Further, despite gross similarities, there is the possibility that there are significant differences between *Rds/Rds* and stem cell–derived photoreceptors.

The purpose of the present study was to determine whether photoreceptor cells that lack an extended outer segment generate visual signals that propagate through the retina and support vision. Then if *Rds/Rds* photoreceptor cells can support vision, the aim was to establish the limitations that lack of a fully formed outer segment places on vision.

Rds photoreceptor cells gradually degenerate so that rods and cones are absent by 1 year of age (Rds^{P365}); however, at postnatal day 90 (Rds^{P90}), ~60% of the photoreceptor cells are retained.[25] We compared retinal function and visual behavioral responses of C3H wild-type (positive control), 90-day-old *Rds* (Rds^{P90}), and 365-day-old *Rds* mice (Rds^{P365}; negative control). The presence of light-evoked responses of the outer retina was tested by electroretinography. Retinal signals to the brain were measured by multielectrode array recording of retinal ganglion cells. Quality of vision (acuity and contrast sensitivity) was tested using two distinct visual behaviors: optokinetic tracking responses and a visual water task discrimination test. Finally, we used a running wheel assay to determine the lowest luminance that supports vision to augment mobility.

Methods

All experiments were performed in accordance with the ARVO Statement for the Use of Animals in Ophthalmic and Vision Research, and were approved by the University of Iowa Animal Care and Use Review. $C3H^{rd1}$ (C3H/HeJ), *Rds* (C3A.BLiA-$Pde6b^{+}$.O20-$Prpb2^{Rds}$/J), and wild-type mice on the same background (C3A.BLiA-$Pde6b^{+}$/J) were from Jackson Laboratories (Bar Harbor, ME).[26] Mice were kept on a daily 12-hour light–dark cycle and provided with food and water ad libitum. Measurements of light were taken using an IL1700 Radiometer (International Light Technologies, Peabody, MA).

Photoreceptor Morphology

Photoreceptor morphology was assessed by histology, immunohistochemistry (IHC), and electron microscopy. Assessment of *Rds/Rds* photoreceptors was by comparison of wild-type, Rds^{P90}, and Rds^{P365} retinas. Assessment of stem cell integration and morphology was conducted in $C3H^{rd1/rd1}$ retinas. Adult dsRed mouse dermal fibroblasts were induced to pluripotency by retroviral transduction with Oct4, Sox4, c-Myc, and KLF4. A photoreceptor-enriched pool of retinal precursor cells was generated using our previously published differentiation protocol and transplanted into the subretinal space of 3-week-old mice; eyes were harvested 21 days later.[7]

For both histology and IHC, eyes were harvested, fixed in 4% paraformaldehyde, and embedded in acrylamide/optimal cutting temperature solution (Ted Pella, Redding, CA), before 7-μm sections were collected using a CM1800 cryostat (Leica, Buffalo Grove, IL). For histology, retinas were stained with hematoxylin and eosin.[27] For IHC, retinas were labeled with 4′,6-diamidino-2-phenylindole (DAPI) to identify nuclei (Vector Labs, Burlingame, CA) and one or more antibodies against dsRed to identify transplanted cells, Rom1, or rhodopsin (RetP1; all from Sigma-Aldrich, St. Louis, MO). Photographs were taken using a BX41 microscope (Olympus, Center Valley, PA) with a SPOT-RT digital camera (Diagnostic Instruments, Sterling Heights, MI).

For electron microscopy, wild-type and Rds^{P90} eyes were processed and labeled with uranyl acetate and lead citrate, as previously described. Images were recorded at ×80 magnification with a transmission electron microscope (JEM-1230; JEOL, Tokyo, Japan) equipped with a 2K × 2K charge coupled device camera (USC1000; Gatan, Inc., Warrendale, PA).

Electroretinogram

Electroretinograms were recorded in dark-adapted wild-type ($n = 8$), Rds^{P90} ($n = 16$), and Rds^{P365} ($n = 8$) mice using an Espion E2 system (Diagnosys, Westford, MA). Mice were anesthetized with ketamine:xylazine (100:20 mg/kg), pupils dilated with Tropicamide 1% (Falcon Pharma, Fort Worth, TX), and corneas moistened using GenTeal (Novartis, New York, NY). Animals were positioned on a temperature-regulated platform and electrodes placed for corneal contact, midline subdermal reference, and ground. Responses to five 4-ms flashes at 25 $cd \cdot s \cdot m^{-2}$ were recorded on a dark background, with interstimulus interval of 60 seconds. For statistical analysis between wild type and Rds^{P90}, b-wave amplitude was compared by two-tailed Mann-Whitney test.

Retinal Ganglion Cell Recording

Light-evoked responses of retinal ganglion cells were recorded from C3H Rds^{P90} and C57BL/6J wild-type retinas ($n = 4$) using multielectrode array techniques as previously reported.[28,29] Dark-adapted retinas were placed ganglion cell layer down onto a multielectrode array with 10-μm contacts at 200-μm spacing (Multichannel Systems, Reutlingen, Germany). The array was mounted on a microscope (Axioplan; Zeiss, Gottingen, Germany) and perfused with 36°C to 37°C oxygenated Ringer medium at 2.5 to 4 mL/min (in mM: 124 NaCl, 2.5 KCl, 2 $CaCl_2$, 2 $MgCl_2$, 1.25 NaH_2PO_2, 26 $NaHCO_3$, and 22 glucose).[30,31] Preparations were stabilized for 1 hour before testing (Bionic Technologies, Salt Lake City, UT).[28] Full-field 1-second flash stimuli were displayed at 5-second intervals, and responses were averaged over 10 trials. Action potential (spike) waveforms accepted for analysis were ≥60 μV in amplitude and ≥1.85 times the root mean square of the background signal. Responses from different cells on the same electrode were distinguished by supervised principle components analysis (PowerNAP, Neuroshare or Offline Sorter; Plexon, Dallas, TX). Accepted data demonstrated a refractory period of >1 ms (typically 2–5 ms) and did not display recognizable noise patterns (60 Hz, >10 kHz transients, or sinusoidal oscillations).[32] Light-evoked responses were identified by an increase in action potentials occurring within the 2 seconds starting from stimulus on (ON and OFF response). Comparison of the number of cells having no identifiable response to light and change in the number of cells of a given type was by two-tailed unequal variance *t*-test.

Optokinetic Responses

The optokinetic response was measured in wild-type, Rds^{P90}, and Rds^{P365} mice ($n = 6$ each) using an OptoMotry system according to previously described methods (Cerebral Mechanics, Lethbridge, AB Canada).[33] Mice were placed onto the elevated platform and presented with a vertically oriented sine wave grating rotating at 12°/s using a direction-randomized "staircase" paradigm. The between-stimulus "blank" was an equal-luminance gray homogenous surround (152 cd/m^2). In tests, either contrast was fixed and acuity tested, or grating was fixed and contrast sensitivity tested. Tracking head movements were scored by a genotype-masked observer. Where no response was observed, an animal was tested at least 10 times at the lowest spatial frequency and maximal contrast. Wild-type and Rds^{P90} data were fitted with a dose–response function in Prism (GraphPad, La Jolla, CA). Due to the limited response range of Rds^{P90} mice, comparison of acuity was made at 100% contrast by two-tailed paired *t*-test.

Visual Water Task

Visual acuity and contrast sensitivity were tested in wild-type ($n = 5$) and Rds^{P90} mice ($n = 7$) using the Acumen two-choice discrimination visual water task (Cerebral Mechanics).[34] Mice were trained to escape the pool of water by swimming to a platform hidden below the surface of the water. A computer

Investigative Ophthalmology & Visual Science

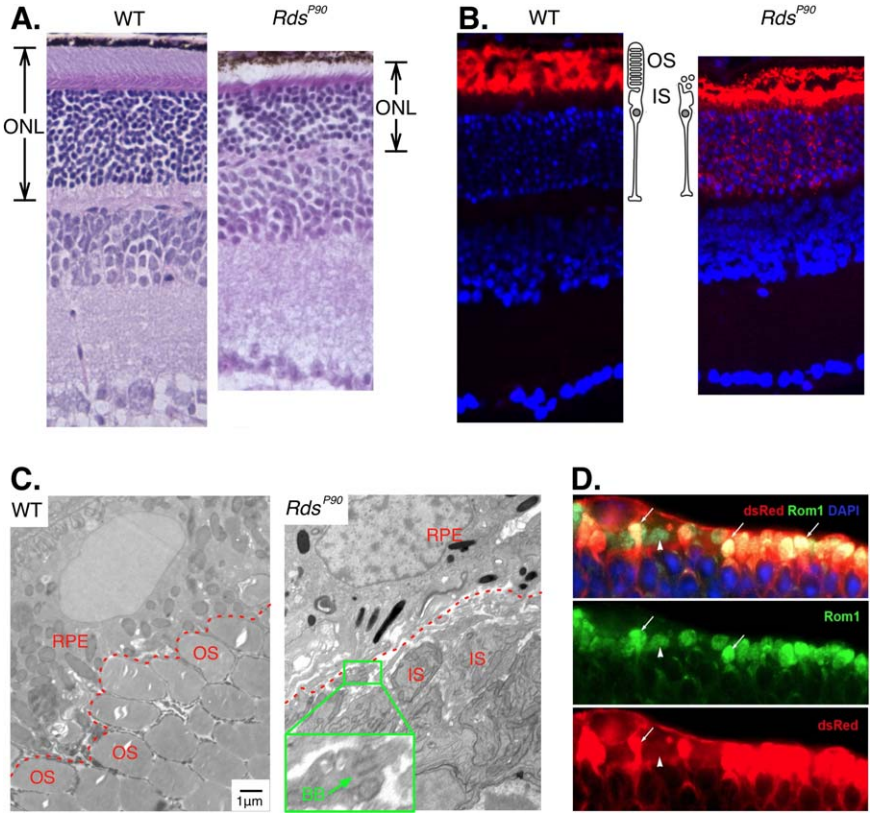

Figure 1. Photoreceptors in *Rds* mice. (**A**) Hematoxylin- and eosin-stained sections show that the Rds^{P90} outer nuclear layer (ONL) is thinner but most photoreceptors are intact. (**B**) Anti-rhodopsin labeling (*red*) shows the efficient compartmentalization of opsin to the photoreceptor outer segments (OS) in wild type, and the lack of a defined outer segment in Rds^{P90}. Nuclei are labeled with DAPI (*blue*). (**C**) Electron microscope images show the stacked discs in outer segments (OS) of wild-type photoreceptor cells. In Rds^{P90} the inner segments (IS) are adjacent to the RPE. No stacked disc-containing structures are apparent. *Inset*: higher-magnification view of an example of a basal body (BB) with a truncated cilium. (**D**) Stem cell–derived photoreceptor cells (dsRed positive) transplanted into a retina with advanced degeneration express outer segment structural proteins (Rom1), but most do not develop an outer segment.

monitor at the end of the pool was used to present a positive or reinforced stimulus that indicated the location of the platform on the left or right of a midline divider. Mice were trained to criterion performance on discrimination between a stationary, vertically oriented, high-contrast sine wave grating (0.12 cycles per degree [cyc/deg]) and uniform gray of the same mean luminance. After training, the threshold to successfully discriminate platform location was determined by systematically increasing the spatial frequency of the positive stimulus. The highest spatial frequency with average $\geq$ 70% correct stimulus/platform discrimination was designated the threshold for that animal. To test contrast sensitivity, contrast was reduced in 10% stages using a low spatial frequency stimulus (0.12 cyc/deg). Comparison was by two-tailed equal variance *t*-test.

Vision-Augmented Mobility

The lowest light level that supported vision useful to mobility was determined according to previously reported methods using a wheel running assay in wild type, Rds^{P90}, and Rds^{P365} ($n = 9$ each).[35] Briefly, mice were individually housed in cages with running wheels, and number of wheel revolutions was recorded against a time stamp using ClockLab (Actimetrics, Wilmette, IL). Cages were mounted in environmental control cabinets with daily cycle of 12-hour light (~180 cd/m^2), 12-hour dark. Separate from the daily light cycle, a 1-hour pulse of light was applied to mice starting 1 hour after daily dark onset. Five light levels of approximately log unit steps between 0.001 and 10 cd/m^2 were applied in a sequence that distributed bright and dim pulses over the course of testing. Change in activity was calculated as percentage of baseline activity measured at the corresponding time on the preceding day for each animal. Significance was determined by a two-tailed *t*-test of activity at the lowest applied luminance, with data at the lowest luminance producing a >10% increase in activity.

Results

Photoreceptor Morphology

In Rds^{P90} mice we observed a deficit in outer segments consistent with previous studies in these mice (Figs. 1A–C). This is similar to the gross morphological deficits of transplanted stem cell–derived photoreceptor precursor cells (Fig. 1D). Photoreceptors are absent in Rds^{P365} mice (Supplementary Fig. S1).

Electroretinography

In the wild-type electroretinogram, a dark-adapted 25 cd · s · m^{-2} flash generated high-amplitude a- and b-waves (Fig. 2). In Rds^{P90} mice, the response to this stimulus had no measurable a-wave and significantly reduced b-wave ($P < 0.005$), comparable to a wild-type response to a 0.001 cd · s · m^{-2} stimulus. In Rds^{P365} mice that had lost all rods and cones, the electroretinogram was nonrecordable.

Investigative Ophthalmology & Visual Science

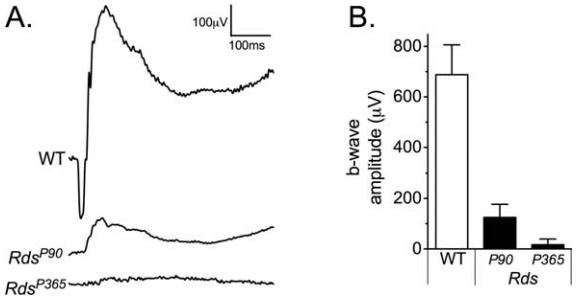

Figure 2. Electroretinogram measurement of gross retinal function. (**A**) Representative electroretinogram waveforms are shown for wild-type, *Rds*^{P90}, and *Rds*^{P365} mice. (**B**) Mean and standard deviation of the b-wave amplitude to a dark-adapted bright flash or "combined maximal response" stimulus is shown for groups of animals.

Retinal Ganglion Cell Recording

Rds^{P90} mice exhibited light-evoked responses in diverse types of retinal ganglion cells (Fig. 3). A 1-second full-field illumination generates characteristic responses in several types of retinal ganglion cells in mouse retinas, including but not limited to cells with ON, sustained-ON, OFF, and ON–OFF responses.[29] The time course of action potential firing in *Rds*^{P90} mice shows that residual photoreceptor function supports light-evoked responses in these distinct groups of retinal ganglion cell types. However, in *Rds*^{P90} retinas, there was (1) a dramatic reduction in the number of ON responses observed ($P = 0.006$) and (2) a significant decrease in the number of cells in which we could identify or reliably distinguish a response to light ($P < 0.05$: cells with an identifiable response to light versus cells identified by baseline action potential activity). Despite this, the mean amplitude of response to light across all cells (responding and nonresponding) was not different ($P = 0.39$).

Optokinetic Responses

Rds^{P90} mice had an optokinetic tracking response but with acuity and contrast thresholds that were reduced compared to those in wild type (Fig. 4). C3H wild-type mice were able to track low contrast and relatively small grating size stimuli.

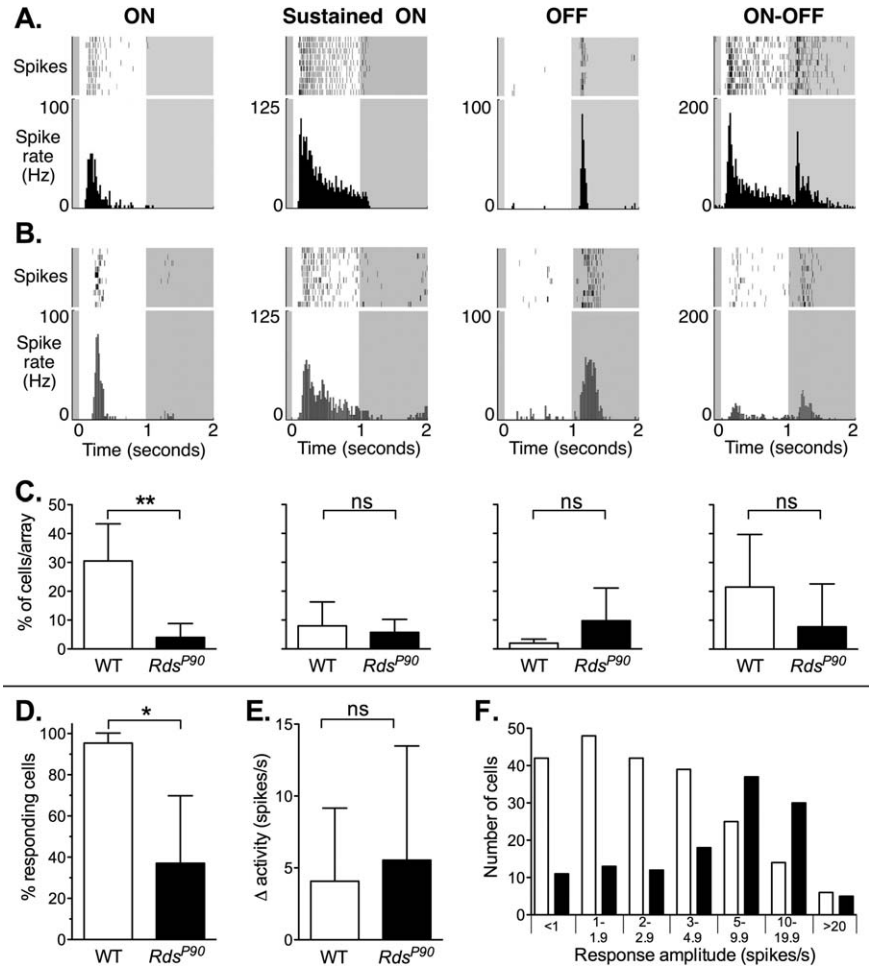

Figure 3. Light-evoked responses of retinal ganglion cells in wild-type and *Rds*^{P90} mice. (**A–C**) Responses are shown in *columns* for ON, sustained ON, OFF, and ON–OFF types of retinal ganglion cells. Example 10-trial raster plots and corresponding peristimulus time histograms are shown for these retinal ganglion cell types in (**A**) wild-type and (**B**) *Rds*^{P90} mice. Timing of the 1-second full-field flash of light is indicated by *white background*. Note that for a given response type, the scale is the same for both wild type and *Rds*^{P90}, but scales are different for each cell type. (**C**) The mean percentage of cells of a given type is shown *below* the histograms (mean and SD per array). (**D**) The percentage of cells identified by baseline action potential activity that had an identifiable response to light is shown for wild-type and *Rds*^{P90} retinas (mean and SD per array). (**E**) The amplitude of change in activity is shown for wild type and *Rds*^{P90} (mean and SD of all cells with an identified response to light). (**F**) The distribution of response amplitudes is shown for wild type and *Rds*^{P90}. Cells are grouped in bins of change in spike rate. Note that the distribution of amplitudes is not Gaussian, so bin sizes are not equal.

Investigative Ophthalmology & Visual Science

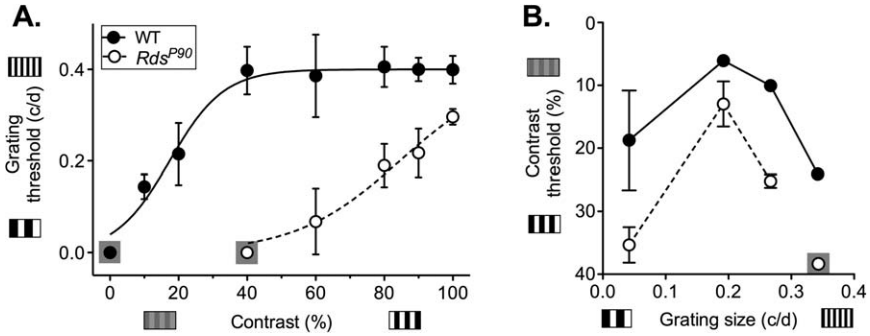

Figure 4. Optokinetic tracking responses. The threshold for tracking responses (mean and SD) in an optokinetic test is shown for (**A**) acuity tested at fixed contrast levels and (**B**) contrast sensitivity tested at fixed grating sizes (cyc/deg). Grating size is the width of the *vertical bars* presented, in cyc/deg. Contrast is the difference in shading between the *light* and *dark bars* of the stimulus. Where no animals responded to a stimulus, data point is shown on a *gray square*.

Contrast did not impact the smallest detectable grating until it was lower than 40% ($P = 0.94$). However, thresholds for contrast sensitivity were dependent on grating size, with peak performance at 0.192 cyc/deg. In Rds^{P90} mice, optokinetic tracking response thresholds were reduced in terms of both contrast sensitivity and acuity. The deficit in acuity at 100% contrast was significant but not pronounced ($P < 0.0001$). However, acuity deteriorated at reduced contrast levels. Rds^{P365} mice with no rods or cones failed to track even a low spatial frequency and maximal-contrast stimulus (0.042 cyc/deg at 100% contrast).

Visual Water Task

Although performance was reduced compared to that in wild type, Rds^{P90} mice were able to discriminate between a sine wave grating against an equal-luminance gray stimulus in the visual water task (Fig. 5). When we compared the threshold responses of individual wild-type and Rds^{P90} mice, acuity and contrast sensitivity were significantly reduced (acuity $P < 0.0001$; contrast sensitivity $P = 0.036$).

Vision-Augmented Mobility

Vision in Rds^{P90} mice was also sufficient to enhance mobility tested by running wheel use (Fig. 6). The lowest radiance that would support vision sufficient to augment this task in wild-type mice was 0.01 cd/m^2 ($P = 0.0001$). Visual function in Rds^{P90} mice was also sufficient to augment wheel running, but only at higher luminances (10 cd/m^2; $P = 0.001$). As expected, in Rds^{P365} mice that had no rods or cones, there was no augmented wheel running at any luminance. Therefore, Rds^{P90} mice show a 2 to 3 log unit loss of sensitivity for vision in dim light compared to wild type.

Discussion

Previous studies have shown that when stem cell–derived photoreceptor cells are introduced to a degenerating retina, a large portion of the cells do not develop extended outer segments.[12] In patients, therapeutic use is likely to be directed

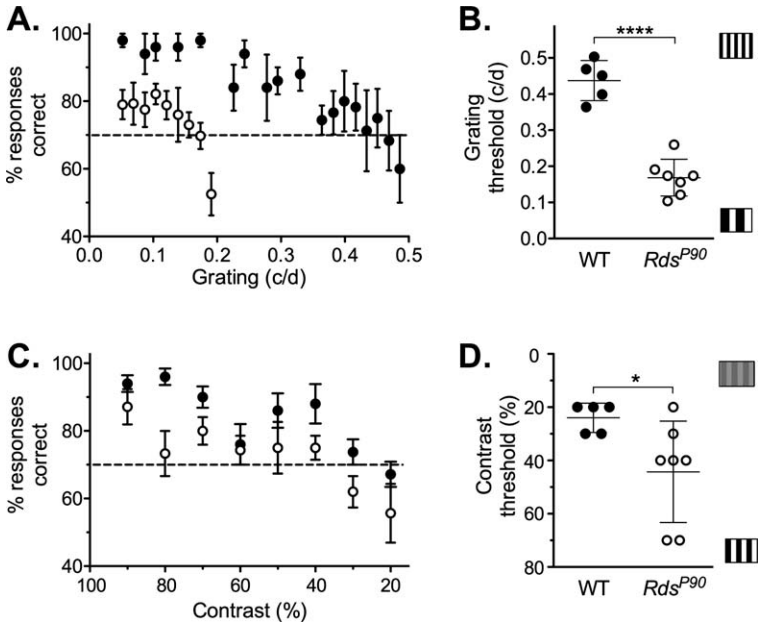

Figure 5. Visual water task. Performance in the stimulus discrimination–based visual water task test is shown for wild-type and Rds^{P90} mice. The percent of trials in which animals positively identified the stimulus versus an equal-luminance control gray screen is shown for (**A**) stimuli with different spatial frequencies and (**C**) stimuli with different levels of percent contrast. Data points are the mean of wild-type and Rds^{P90} mice. Performance below 70% correct indicates the animals could not distinguish the positive stimulus from the equal-luminance gray screen. The threshold for individual animals is then shown for (**B**) spatial frequency or grating (acuity) and (**D**) contrast sensitivity.

Investigative Ophthalmology & Visual Science

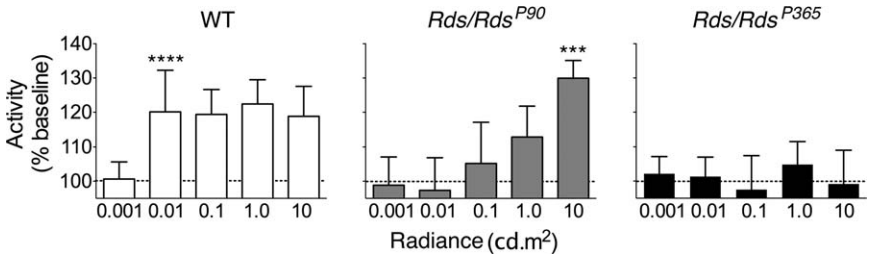

FIGURE 6. Vision augmented wheel running. The effect of light on wheel running activity is shown for wild-type, *Rds*^{P90}, and *Rds*^{P365} mice at different luminance levels. Responses are defined as a percentage of baseline activity in complete darkness. Significance is indicated for the dimmest light level generating a increase in activity (****$P < 0.0001$; ***$P < 0.001$).

at severely degenerated retinas. The purpose of this study was to determine whether lack of a fully formed outer segment precludes a useful contribution to vision. We studied retinal and visual function in *Rds*^{P90} mice because their photoreceptor cells have a grossly similar structural deficit.

We first confirmed that there are clear similarities in gross structure of *Rds* and stem cell–derived photoreceptor cells, although significant differences may exist.[16,18,19,22,23] We then demonstrated that *Rds*^{P90} photoreceptor cells generated light-evoked responses that propagated through the retina and supported a variety of visual tasks. Quality of vision was sufficiently good to have measurable acuity in light conditions consistent with a typical visual environment (indoor lighting). Therefore, our findings demonstrate that at least in *Rds*^{P90} mice, lack of a fully formed outer segment does not preclude a useful contribution to vision.

Visual Signal Generation and Transmission

To determine whether photoreceptor cells lacking extensive outer segments could plausibly support vision, we measured light-evoked responses in the retina of *Rds*^{P90} mice. Consistent with previous studies, we recorded a b-wave with reduced amplitude.[24,36] The b-wave is generated by second-order neurons that are postsynaptic to the photoreceptor cells. The amplitude of the electroretinogram b-wave (15% of wild type) was much better than would be estimated from the level of opsin (~3%).[16] This points to compensatory signal gain in the synaptic output of the photoreceptor cells and/or the response of bipolar cells to synaptic input from the photoreceptor cells.

Importantly, we found that this outer retinal response to light was transmitted through the retina to retinal ganglion cells. Light-evoked responses were generated in diverse physiological types of retinal ganglion cells. This is consistent with the variety of retinal output in a normal retina and the diversity of visual capabilities that these different retinal ganglion cell types support.[29,37] Although there was no difference in mean amplitude of responses, a significant number of cells lacked identifiable responses to light. The basis for this deficit and shift in response amplitudes is not clear, but retinal pathology or reduced photon capture may cause some circuits to fall below detection threshold while the response of others is increased.[38,39]

Quality and Limitations of Vision in *Rds*^{P90} Mice

To determine whether the observed retinal function would support useful vision, we measured three different visual behaviors. Together these tests showed that *Rds*^{P90} mice retain useful vision, but with limitations.

Optokinetic responses test the ability of an animal to track a moving stimulus, and depend on retinal input to the accessory optic system.[33] *Rds*^{P90} mice retained optokinetic responses, and at optimal grating sizes, performance was nearly as good as that of wild type.[33] However, performance was more severely degraded than in wild type with suboptimal grating sizes and as contrast was reduced. The visual water task tests the ability of an animal to discern a stationary image and depends on retinal input to the dorsal lateral geniculate nucleus, superior colliculus, and/or pretectum.[40,41] *Rds*^{P90} mice were also able to distinguish a vertical sine wave grating from an equal-luminance stimulus; but again, acuity and contrast sensitivity were reduced. Finally, visual function in *Rds*^{P90} mice was sufficient to enhance mobility (use of a running wheel), but not at very low luminances.[35] Importantly, the 10 cd/m^2 luminance supporting vision useful to mobility in *Rds*^{P90} mice approximates twilight, so typical daytime or room lighting levels would support vision (100–100,000 cd/m^2).

The level of light required for vision-augmented mobility was increased by 2 to 3 orders of magnitude. This is only marginally greater than the reduction in opsin that captures and initiates the response to light.[16,23] Therefore, the absence of extensive outer segments appears to determine the lowest light level that supports vision primarily because it limits the capacity to capture light. It is also possible that this decrease in photon capture accounts for the reduced capacity to discriminate detail and contrast, and that performance would increase as luminance increases.[42]

Basis for Quality of Vision

The quality of retinal and visual function in *Rds*^{P90} mice points to signal gain plasticity in the visual circuits, allowing relatively poor photon capture capacity to generate a useful visual signal. Plasticity in cortical circuits may largely account for this functional disparity.[43,44] However, we found evidence of signal gain at the level of the photoreceptor and/or second-order neurons: The electroretinogram b-wave had higher amplitude than predicted by the reported level of opsin expression.[16,23] If we assume that levels of opsin determine photon capture capacity (3% of wild type), then we would predict a much smaller electroretinogram b-wave (3% of wild-type b-wave = 21 μV). Instead we observed a mean electroretinogram b-wave at ~18% of wild type (125 μV).

Translational Relevance

This and other studies have shown that stem cell–derived photoreceptor cells introduced to a degenerating retina often do not give rise to fully formed outer segments.[12] The photoreceptor cells in the *Rds* retina have a similar structural deficit.[16–21] We showed that despite this structural deficit, photoreceptor cells in *Rds*^{P90} mice can support useful vision. This suggests that the majority of transplanted stem cell–

derived photoreceptor cells have the potential to support a meaningful gain in vision, even if they do not develop fully formed outer segments. Further, in inherited disease where outer segments are dysmorphic, such as Bardet-Biedl syndrome,[27] therapy that promotes cell survival at the expense of outer segment structure may protect quality of vision. Our findings also point to the importance of mechanisms for compensation in visual signal pathways. Manipulating these mechanisms may provide an approach for maximizing therapeutic replacement of photoreceptor function (whether gene, cell, or prosthetic therapy).

Acknowledgments

We thank Michael Andrews, Arlene V. Drack, Markus H. Kuehn, and Megan Riker for assistance.

Supported by the Howard Hughes Medical Institute (EMS), Stephen A. Wynn Institute for Vision Research (ST, BAT, SFS, EMS), National Institutes of Health Grant 1DP2OD007483 (BAT), Foundation Fighting Blindness (EMS, BAT), and Grousbeck Family Foundation (ST, BAT, SFS, EMS).

Disclosure: **S. Thompson**, None; **F.R. Blodi**, None; **S. Lee**, None; **C.R. Welder**, None; **R.F. Mullins**, None; **B.A. Tucker**, None; **S.F. Stasheff**, None; **E.M. Stone**, None

References

1. Nowak JZ. Age-related macular degeneration (AMD): pathogenesis and therapy. *Pharmacol Rep*. 2006;58:353–363.
2. Berson EL. Retinitis pigmentosa. *Invest Ophthalmol Vis Sci*. 1993;34:1659–1676.
3. Simunovic MP, Moore AT. The cone dystrophies. *Eye*. 1998; 12(pt 3b):553–565.
4. Huberman AD, Niell CM. What can mice tell us about how vision works? *Trends Neurosci*. 2011;34:464–473.
5. Masland RH. Neuronal diversity in the retina. *Curr Opin Neurobiol*. 2001;11:431–436.
6. MacLaren RE, Pearson RA, MacNeil A, et al. Retinal repair by transplantation of photoreceptor precursors. *Nature*. 2006; 444:203–207.
7. Tucker BA, Park IH, Qi SD, et al. Transplantation of adult mouse iPS cell-derived photoreceptor precursors restores retinal structure and function in degenerative mice. *PLoS ONE*. 2011;6:e18992.
8. Barber AC, Hippert C, Duran Y, et al. Repair of the degenerate retina by photoreceptor transplantation. *Proc Natl Acad Sci U S A*. 2013;110:354–359.
9. Gonzalez-Cordero A, West EL, Pearson RA, et al. Photoreceptor precursors derived from three-dimensional embryonic stem cell cultures integrate and mature within adult degenerate retina. *Nat Biotechnol*. 2013;31:741–747.
10. Klassen HJ, Ng TF, Kurimoto Y, et al. Multipotent retinal progenitors express developmental markers, differentiate into retinal neurons, and preserve light-mediated behavior. *Invest Ophthalmol Vis Sci*. 2004;45:4167–4173.
11. Lakowski J, Han YT, Pearson RA, et al. Effective transplantation of photoreceptor precursor cells selected via cell surface antigen expression. *Stem Cells*. 2011;29:1391–1404.
12. Singh MS, Charbel Issa P, Butler R, et al. Reversal of end-stage retinal degeneration and restoration of visual function by photoreceptor transplantation. *Proc Natl Acad Sci U S A*. 2013;110:1101–1106.
13. Pearson RA, Barber AC, Rizzi M, et al. Restoration of vision after transplantation of photoreceptors. *Nature*. 2012;485:99–103.
14. Del Debbio C, Peng X, Xiong H, Ahmad I. Adult ciliary epithelial stem cells generate functional neurons and differentiate into both early and late born retinal neurons under non-cell autonomous influences. *BMC Neurosci*. 2013;14:1–14.
15. Demontis GC, Aruta C, Comitato A, De Marzo A, Marigo V. Functional and molecular characterization of rod-like cells from retinal stem cells derived from the adult ciliary epithelium. *PLoS ONE*. 2012;7:e33338.
16. Agarwal N, Nir I, Papermaster DS. Opsin synthesis and mRNA levels in dystrophic retinas devoid of outer segments in retinal degeneration slow (rds) mice. *J Neurosci*. 1990;10:3275–3285.
17. Chang B, Hawes NL, Hurd RE, Davisson MT, Nusinowitz S, Heckenlively JR. Retinal degeneration mutants in the mouse. *Vision Res*. 2002;42:517–525.
18. Farjo R, Naash MI. The role of Rds in outer segment morphogenesis and human retinal disease. *Ophthalmic Genet*. 2006;27:117–122.
19. Jansen HG, Sanyal S. Development and degeneration of retina in rds mutant mice: electron microscopy. *J Comp Neurol*. 1984;224:71–84.
20. Nir I, Agarwal N, Papermaster DS. Opsin gene expression during early and late phases of retinal degeneration in rds mice. *Exp Eye Res*. 1990;51:257–267.
21. Sanyal S, Jansen HG. Absence of receptor outer segments in the retina of *rds* mutant mice. *Neurosci Lett*. 1981;21:23–26.
22. Jansen HG, Sanyal S, De Grip WJ, Schalken JJ. Development and degeneration of retina in rds mutant mice: ultraimmunohistochemical localization of opsin. *Exp Eye Res*. 1987;44:347–361.
23. Schalken JJ, Janssen JJ, De Grip WJ, Hawkins RK, Sanyal S. Immunoassay of rod visual pigment (opsin) in the eyes of rds mutant mice lacking receptor outer segments. *Biochim Biophys Acta*. 1985;839:122–126.
24. Reuter JH, Sanyal S. Development and degeneration of the retina in *rds* mutant mice: the electroretinogram. *Neurosci Lett*. 1984;48:231–237.
25. Sanyal S, De Ruiter A, Hawkins RK. Development and degeneration of retina in *rds* mutant mice: light microscopy. *J Comp Neurol*. 1980;194:193–207.
26. Lucas RJ, Freedman MS, Munoz M, Garcia-Fernandez JM, Foster RG. Regulation of the mammalian pineal by non-rod, non-cone, ocular photoreceptors. *Science*. 1999;284:505–507.
27. Davis RE, Swiderski RE, Rahmouni K, et al. A knockin mouse model of the Bardet-Biedl syndrome 1 M390R mutation has cilia defects, ventriculomegaly, retinopathy, and obesity. *Proc Natl Acad Sci U S A*. 2007;104:19422–19427.
28. Stasheff SF. Emergence of sustained spontaneous hyperactivity and temporary preservation of OFF responses in ganglion cells of the retinal degeneration (rd1) mouse. *J Neurophysiol*. 2008; 99:1408–1421.
29. Stasheff SF, Shankar M, Andrews MP. Developmental time course distinguishes changes in spontaneous and light-evoked retinal ganglion cell activity in rd1 and rd10 mice. *J Neurophysiol*. 2011;105:3002–3009.
30. Tian N, Copenhagen DR. Visual deprivation alters development of synaptic function in inner retina after eye opening. *Neuron*. 2001;32:439–449.
31. Meister M, Pine J, Baylor DA. Multi-neuronal signals from the retina: acquisition and analysis. *J Neurosci Methods*. 1994;51: 95–106.
32. Segev R, Goodhouse J, Puchalla J, Berry MJ II. Recording spikes from a large fraction of the ganglion cells in a retinal patch. *Nat Neurosci*. 2004;7:1154–1161.
33. Douglas RM, Alam NM, Silver BD, McGill TJ, Tschetter WW, Prusky GT. Independent visual threshold measurements in the two eyes of freely moving rats and mice using a virtual-reality optokinetic system. *Vis Neurosci*. 2005;22:677–684.

34. Prusky GT, West PW, Douglas RM. Behavioral assessment of visual acuity in mice and rats. *Vision Res*. 2000;40:2201–2209.
35. Thompson S, Philp AR, Stone EM. Visual function testing: a quantifiable visually guided behavior in mice. *Vision Res*. 2008;48:346–352.
36. Schlichtenbrede FC, da Cruz L, Stephens C, et al. Long-term evaluation of retinal function in Prph2Rd2/Rd2 mice following AAV-mediated gene replacement therapy. *J Gene Med*. 2003;5:757–764.
37. Farrow K, Masland RH. Physiological clustering of visual channels in the mouse retina. *J Neurophysiol*. 2011;105:1516–1530.
38. Buldyrev I, Puthussery T, Taylor WR. Synaptic pathways that shape the excitatory drive in an OFF retinal ganglion cell. *J Neurophysiol*. 2012;107:1795–1807.
39. Dunn FA, Doan T, Sampath AP, Rieke F. Controlling the gain of rod-mediated signals in the mammalian retina. *J Neurosci*. 2006;26:3959–3970.
40. Prusky GT, Douglas RM. Characterization of mouse cortical spatial vision. *Vision Res*. 2004;44:3411–3418.
41. Ecker JL, Dumitrescu ON, Wong KY, et al. Melanopsin-expressing retinal ganglion-cell photoreceptors: cellular diversity and role in pattern vision. *Neuron*. 2010;67:49–60.
42. Lythgoe JN. Visual pigments and environmental light. *Vision Res*. 1984;24:1539–1550.
43. Davis GW. Homeostatic control of neural activity: from phenomenology to molecular design. *Annu Rev Neurosci*. 2006;29:307–323.
44. Nelson SB, Turrigiano GG. Strength through diversity. *Neuron*. 2008;60:477–482.

Investigative Ophthalmology & Visual Science